

# EXPLORING THE TEMPORAL AND SPATIAL VARIATION OF THE NET PRIMARY PRODUCTIVITY IN TROPICAL ISLANDS USING CMIP6 MODEL: A CASE STUDY OF HAINAN ISLAND, CHINA

HAN, N. L.<sup>1,3\*</sup> – LIU, Q. Y.<sup>2,3</sup>

<sup>1</sup>*School of Geography and Tourism, Huizhou University, Huizhou 516007, China*

<sup>2</sup>*School of Resource and Environmental Science, Wuhan University, Wuhan 430072, China*

<sup>3</sup>*School of Public Administration, Hainan University, Haikou 570228, China*

*\*Corresponding author  
e-mail: nlhan@hainanu.edu.cn*

(Received 7<sup>th</sup> Nov 2024; accepted 27<sup>th</sup> Feb 2025)

**Abstract.** Vegetation net primary productivity (NPP) is a key ecological indicator for evaluating ecosystem services. Understanding how future climate change will impact NPP in Hainan Island is essential for promoting the sustainable development of ecosystem services on tropical islands. In this study, we employed an improved version of the Carnegie-Ames-Stanford Approach (CASA) model to analyze the spatial and temporal patterns of NPP on Hainan Island from 2000 to 2018 and to identify the main factors influencing these changes. To project future NPP trends in 2050, we integrated the Future Land Use Simulation (FLUS) model with climate projections from the Coupled Model Intercomparison Project Phase6 (CMIP6). The key finding of this study as follows: (1) From 2000 to 2018, the average NPP on Hainan Island exhibited an increasing trend, with a significant positive correlation between NPP and climatic factors such as precipitation, solar radiation, and temperature. (2) During the same period, land use changes led to a decline in NPP; however, this negative effect was offset by favorable climate conditions, resulting in an overall increase in NPP of approximately 12.7%. (3) By 2050, under the combined influence of future climate and land use changes, NPP on Hainan Island is projected to a decline across all three climate scenarios. Among them, the SSP2-4.5 scenario demonstrates a moderate mean NPP level, maintaining the functional stability of NPP while aligning with regional development objectives, thereby positioning it as the optimal pathway to support Hainan Island's future sustainable development.

**Keywords:** *net primary productivity (NPP), climate change, land use, SSP-RCPs, CMIP6*

## Introduction

Global climate change and human activities have significant impacts on terrestrial ecosystem services (Liu et al., 2022). For example, environmental disturbances such as fires, pests, and diseases brought about by climate change have degraded ecosystem services and functions of temperate forests (Rawat et al., 2022). Increased extreme weather events has led to a decline in mangrove areas (Wang and Gu, 2021), warming and more frequent ocean heatwaves, has led to a global reduction in coral reefs areas (Camp et al., 2018), and climate change overlaid with human activities have led to a decline in Earth's biodiversity.

Net primary productivity (NPP) refers to the total amount of organic biomass accumulated by green plants per unit time and unit area (Xue et al., 2022). It is a key ecosystem function that directly reflects the carbon sequestration capacity and productivity of vegetation. NPP is influenced by various factors, including vegetation types, climate conditions, and land use. Among these, climate factors such as temperature, precipitation, and solar radiation, and their interactions have particularly

significant impacts on NPP (Cao et al., 2021). For instance, precipitation strongly influences NPP in southwestern tropical rainforests characterized by distinct wet and dry seasons (Linger et al., 2020). In the Pearl River Basin, reduced sunshine duration and lower temperatures have been shown to negatively affect NPP (Li et al., 2022). Similarly, extreme temperatures combined with decreased precipitation lead to reduced NPP in forest ecosystems in the Himalaya (Kumar et al., 2019). Tropical vegetation, in particular, is more vulnerable to productivity losses under increasing climate change pressures compared to ecosystems in mid-to-high latitudes (Yuan et al., 2016). This vulnerability is further compounded by the intensification of extreme climatic events (e.g., droughts and heatwaves) and the saturation threshold of NPP, which introduce substantial uncertainties into the functional stability of tropical ecosystems (Reichstein et al., 2013; Xu et al., 2019; Cao et al., 2021). Therefore, understanding how NPP response to future climate and land use changes is critical for guiding sustainable regional ecological and socio-economic development. Existing NPP estimation models can be broadly categorized into three types: statistical models, parameter models, and process models (Yang et al., 2021). Statistical models often overlook the physiological mechanisms of vegetation, while parameter models require numerous complex parameters that are difficult to obtain due to their intricate physiological mechanisms. In contrast, process model-based on the principle of light energy utilization simplifies vegetation physiological processes, and their vegetation parameters can be obtained from remote sensing data, making them more commonly used for NPP estimation. Among these, widely adopted light energy utilization models include the Carnegie-Ames-Stanford Approach (CASA), the improved CASA model, and GLO-PEM model. The improved CASA model builds upon the original CASA framework and by incorporating China specific NPP data and vegetation characteristics, thereby localizing (or "Sinicizing") static parameters—to Sinicize the static parameters—such as maximum light energy utilization—to better reflect real-world conditions in China (Zhu et al., 2006; Zhu et al., 2007). Based on the improved CASA model, numerous researches have assessed NPP across various spatial scales and regions in China. For example, it has been applied in Northwest China (Li et al., 2021), the Dongting Lake Basin (Zhang et al., 2022a), and Hangzhou City (Li et al., 2021), all of which demonstrated the model's effectiveness and applicability.

Understanding the patterns of historical and future climate change is of great scientific importance for adapting to and mitigating its impacts on NPP. The Coupled Model Intercomparison Project (CMIP), initiated by the Intergovernmental Panel on Climate Change (IPCC), provides a series of future climate scenarios that integrate both socio-economic developments and greenhouse gas trajectories (Jiang et al., 2020).

These scenarios have been widely adopted in research related to future carbon storage (Yang et al., 2020; Wang et al., 2022), runoff estimated (Xue et al., 2024), crop yield projections (Arunrat et al., 2022), and restoration of key ecosystems function (Khelifa et al., 2022). Now in its sixth phase (CMIP6), the project incorporates both Representative Concentration Pathways (RCPs) with Shared Socioeconomic Pathways (SSPs), resulting in eight combined SSP-RCP scenarios. This integrated framework offers a more comprehensive perspective on the interplay between climate change and socio-economic development. Hainan Island is a representative tropical island in China, characterized by a relatively independent ecosystem that is highly sensitive to climate change. In recent year, rapid economic development and intensified human activities have significantly impacted the island's ecosystem services, leading to ecosystem

degradation and a decline in overall ecosystem health (Chiaka et al., 2024). These changes present substantial challenges to the region's sustainable ecological and socio-economic development (Hernández-Delgado, 2015). However, the processes and mechanisms through which climate and land use changes affect NPP on Hainan Island remain insufficiently understood, and limited research has focused on the island's NPP response to future climate and land use scenarios.

In light of this, the present study employs the improved CASA model to assess the NPP on Hainan Island, with the aim of addressing the following key questions: (1) What are the spatial and temporal variations in NPP on Hainan Island from 2000 to 2018, and what are the main factors influencing these changes?(2) How will NPP be distributed under future land use and climate changes scenarios, based on simulations using three climate scenarios: SSP1-2.6, SSP2-4.5, and SSP5-8.5?(3) What sustainable development strategies can be proposed to preserve and enhance NPP functions in response to future climate and land use changes on Hainan Island?

## Materials and methods

### Study area

Hainan Island is situated in a tropical maritime monsoon climate zone (*Fig. 1*), characterized by warm temperatures year-round, with an annual average temperature exceeding 23°C. The region receives substantial precipitation, with annual rainfall averaging over 900 mm. Covering a land area of approximately 34,000 km<sup>2</sup>, the island features a topography dominated by a high central region, including the Wuzhi Mountains (1867 m) and Parrot Ridge, surrounded by descending order such as mountains, hills, tablelands, and plains (with elevations below 200 m). According to land uses from 2018(<https://www.resdc.cn/>), the primary land cover types in Hainan Island were forest land (21,659 km<sup>2</sup>, 62.98%) and cropland (8970 km<sup>2</sup>, 26.08%). By the end of 2020, Hainan's GDP reached 553.239 billion yuan, with a resident population of 10.1234 million and an urbanization rate of 60.7%. As both a designated free trade port and a National Ecological Civilization Pilot area, Hainan faces the dual challenge of promoting economic development while addressing ecological pressures, including shrinking ecological spaces, biodiversity loss, and declining ecosystem service functions.

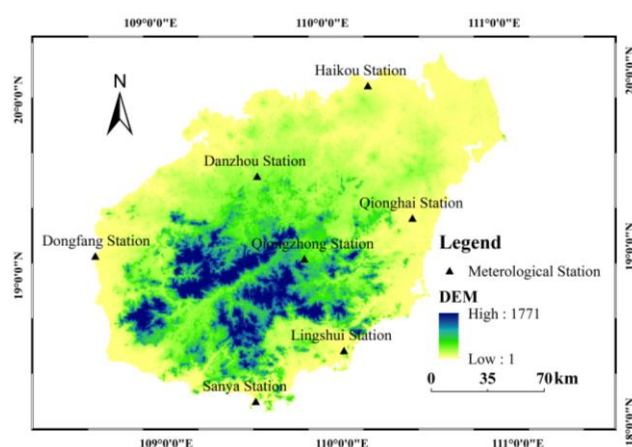


**Figure 1.** Map of the study area

### **Data source and processing**

The data used in this study include historical meteorological data, CMIP6 climate projections, NDVI, land use data, and land use driving factors. Historical meteorological data consist of daily average temperature (°C), daily precipitation (mm), and sunshine duration (hours) from 1991 to 2020, collected from seven meteorological stations on Hainan Island. The average monthly temperature, total precipitation, and sunshine duration for the periods 1991-2000, 2001-2010, and 2011-2020 were used to characterized the monthly meteorological conditions for the year 2000, 2010, and 2018, respectively (*Table 2*). Total solar radiation for Hainan Island was estimated by converting sunshine duration data. , The station-based meteorological observations were then interpolated into 1 km resolution raster data using the Inverse Distance Weighting (IDW) interpolation method.

For future climate projections, three models(BCC-CSM2-MR, MIROC6, and MRI-ESM2-0) were selected due to their high accuracy in simulating climatic variables overChina (Zhang et al., 2022b; Tian et al., 2022). Three future scenarios, SSP1-2.6, SSP2-4.5, and SSP5-8.5, were chosen based on their relevance, with details scenario descriptions available in the literature (Zhang et al., 2019). In this study, the monthly meteorological averagesfrom 2041 to 2050,based on outputs from the three selected models, were used to represent the projected monthly climateconditions in 2050.

The future climate data were first downscaled using the IDW method (Chen et al., 2021), followed by bias correction using the Delta method (Raty et al., 2014; Guo et al., 2016). This process producedmonthly average temperature, total precipitation, and total solar radiation data for the three scenarios: SSP1-2.6, SSP2-4.5, and SSP5-8.5 (*Table 1*).

**Table 1.** List of monthly climate factors in difference periods and scenarios

| <b>Climate factors</b>                             | <b>2000</b> | <b>2010</b> | <b>2018</b> | <b>Historical mean value</b> | <b>2050 SSP1-2.6</b> | <b>2050 SSP2-4.5</b> | <b>2050 SSP5-8.5</b> |
|--|-------------|-------------|-------------|------------------------------|----------------------|----------------------|----------------------|
| Monthly mean temperature (°C)                      | 24.54       | 24.72       | 24.56       | 24.61                        | 26.18                | 26.30                | 26.59                |
| Monthly total precipitation (mm)                   | 149.81      | 151.07      | 159.85      | 153.58                       | 88.75                | 99.25                | 80.20                |
| Monthly total solar radiation (MJ/m <sup>2</sup> ) | 629.12      | 596.55      | 582.49      | 602.72                       | 560.51               | 535.14               | 546.88               |

The Normalized Difference Vegetation Index (NDVI) is defined as the ratio of the difference to the sum of reflectance values between the near-infrared band (NIR) and red band (R), as shown in the following formula:

$$NDVI = (NIR - R) / (NIR + R)$$

The NDVI data for 2000, 2010, and 2018 were obtained from the Resources and Environment Science and Data Centers, with a spatial resolution of 1 km. The NDVI for 2050 was estimated based on land use projections. If the land use of a given pixel remained unchanged between 2018 and 2050, the average NDVI value from 2000 to 2018 was used.If land use changed, the NDVI value from 2018 for that pixel was adopted. Land use data for 2000, 2010, and 2018, with a spatial resolution of 1 km,

included ten categories: cropland, forestland, sparse woodland, shrub, other woodland, grassland, construction land, water, tidal flat, and other land. Future land use changes for 2050 were simulated using the Future Land Use Simulation (FLUS) model. The FLUS Model requires multiple input layers, including: land use data, natural factors (elevation, slope, and distance to the river), transportation factors (distance to general highways, expressways, and towns), and socio-economic factors (permanent resident population and GDP of cities in Hainan Province). Slope were derived from a digital elevation model (DEM), and distance were calculated using the European distance method. Socio-economic factors were obtained from statistical yearbooks and official datasets. All spatial data were converted to the Albers projection coordinate system. *Table 2* provides detailed descriptions data sources and contents.

**Table 2.** Required data and sources in this study

| Data type                               | Content of data  | Data source   | Time of data     |
|---|--|---|------------------|
| Historical meteorological data          | Daily mean temperature, total precipitation, sunshine duration     | <a href="http://data.cma.cn/">http://data.cma.cn/</a>   | 1991-2020        |
| Future climate data                     | Daily mean temperature, total precipitation, total solar radiation | <a href="https://esgf-node.llnl.gov/search/cmip6/">https://esgf-node.llnl.gov/search/cmip6/</a>   | 2041-2050        |
| NDVI                                    | Monthly NDVI (1 km)  | <a href="https://www.resdc.cn/">https://www.resdc.cn/</a>   | 2000, 2010, 2018 |
| Land use data                           | Land use map (1 km)  | <a href="https://www.resdc.cn/">https://www.resdc.cn/</a>   | 2000, 2010, 2018 |
| Driving factors for land use simulation | permanent resident population and GDP of cities in Hainan Province | <a href="http://stats.hainan.gov.cn/tjj/index.html">http://stats.hainan.gov.cn/tjj/index.html</a> | 2020             |
|   | DEM (30 m)   | <a href="http://www.ngcc.cn/ngcc/">http://www.ngcc.cn/ngcc/</a>                                   | 2020             |
|   | Distribution map of river and water bodies                         | <a href="https://www.openstreetmap.org/">https://www.openstreetmap.org/</a>                       | 2020             |
|   | Distribution map of general highways and expressways               | <a href="https://www.openstreetmap.org/">https://www.openstreetmap.org/</a>                       | 2020             |
|   | Distribution map of railways                                       | <a href="https://www.openstreetmap.org/">https://www.openstreetmap.org/</a>                       | 2020             |

## Methods

### Improved CASA

In this study, the improved CASA model was employed to estimate the NPP of Hainan Island. The detailed calculation procedures and model framework has been comprehensively described in previous studies (Zhu et al., 2006, 2007) and are therefore not reiterated here. Based on the parameter localization for the improved CASA model, the finalized static parameters specific to Hainan Island are listed in *Table 3*.

**Table 3.** Localized parameters for Improved CASA model

| Land-use types    | $NDVI_{max}$ | $NDVI_{min}$ | $SR_{max}$ | $SR_{min}$ | $\epsilon_{max}$ |
|-------------------|--------------|--------------|------------|------------|------------------|
| Cropland          | 0.848        | 0.023        | 13.286     | 1.050      | 0.542            |
| Forestland        | 0.888        | 0.023        | 16.857     | 1.050      | 0.985            |
| Shrub             | 0.856        | 0.023        | 12.889     | 1.050      | 0.429            |
| Sparse woodland   | 0.852        | 0.023        | 12.514     | 1.050      | 0.542            |
| Other woodland    | 0.864        | 0.023        | 12.889     | 1.050      | 0.638            |
| Grassland         | 0.852        | 0.023        | 13.286     | 1.050      | 0.542            |
| Water             | 0.836        | 0.023        | 13.706     | 1.050      | 0.542            |
| Tidal flat        | 0.788        | 0.023        | 8.804      | 1.050      | 0.542            |
| Construction land | 0.832        | 0.023        | 10.111     | 1.050      | 0.542            |
| Other land        | 0.648        | 0.023        | 4.435      | 1.050      | 0.542            |

### FLUS model

The FLUS model primarily comprises three components: land use demand projection based on System Dynamics (SD), a probability-of-occurrence calculation using an artificial neural network-based (ANN), and a self-adaptive inertia and competition mechanism (Liu et al., 2017). In this study, 10% of the 2018 land use data were randomly selected as the training samples. The ANN was configured with 10 hidden layers, and normalized driving factor was employed to calculate the probability of land use -occurrence in Hainan Island for the year 2050. Subsequently, a Markov chain model was used to project land use demand for each category in 2050 and to compute the difference from actual land use in order to determine the adaptive inertia coefficient. Finally, a roulette wheel selection mechanism was applied to assign the final land use types to each grid cell, resulting in the land use simulation for 2050. Model parameters, such as neighborhood impact factors and conversion cost were determined with reference to previous FLUS-based studies in Hainan Island (Han et al., 2022).

## Results

### *Spatial and temporal changes of NPP in Hainan Island from 2000 to 2018*

The spatial distribution of NPP on Hainan Island exhibits a distinct pattern of high values in the central region and lower values in the surrounding areas (Fig. 2). From 2000 to 2018, the average annual NPP was  $1330.03\text{gC m}^{-2}\text{ a}^{-1}$ , with a total NPP of  $0.0457\text{PgC m}^{-2}\text{ a}^{-1}$ . Over this period, NPP showed a consistent upward trend, with average values of  $1263.31\text{gC m}^{-2}\text{ a}^{-1}$  in 2000,  $1302.82\text{gC m}^{-2}\text{ a}^{-1}$  in 2010, and  $1423.96\text{gC m}^{-2}\text{ a}^{-1}$  in 2018. Overall, NPP increased by approximately 12.72% from 2000 to 2018.

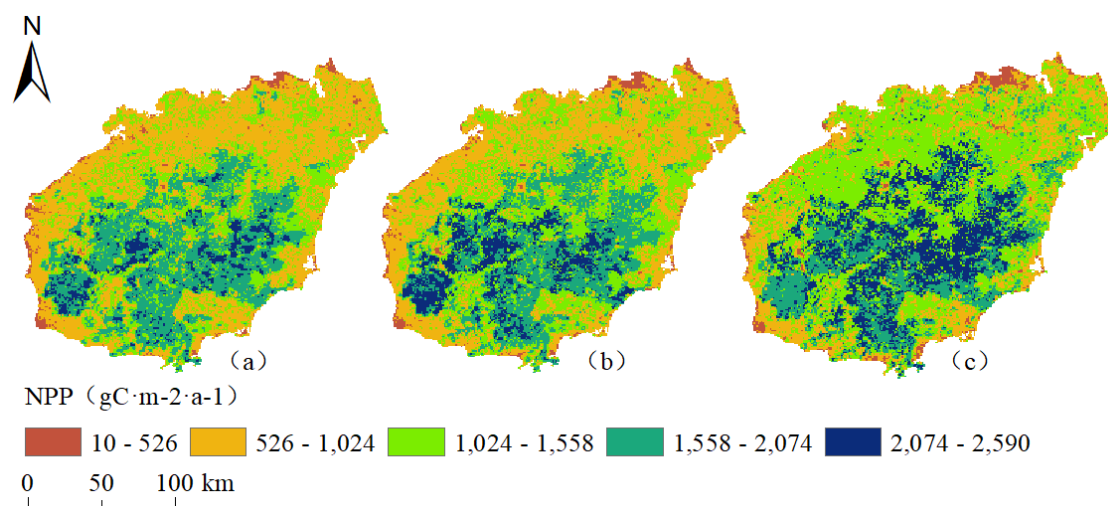


**Figure 2.** NPP distribution map of Hainan Island in different periods, in 2000 (a), in 2010 (b), in 2018 (c)

Spatial variations in NPP on Hainan Island from 2000 to 2018 indicate that NPP growth was predominantly concentrated in the central and western regions. This increase is largely attributed to the designation of the central mountainous area as a National key Ecological Function Area in 2000. Following this designation, the

government implemented a series of ecological protection measures, including restricting development in mountainous areas, promoting afforestation, and encouraging grassland restoration. These initiatives effectively reduced deforestation and limited anthropogenic disturbances. Since 2011, further ecological restoration efforts, such as large-scale afforestation, replanting of low-efficiency forests, and the transformation or withdrawal of artificial forest, have contributed to the gradual recovery of tropical rainforests in the central region, thereby continuously enhancing NPP (Chiaka et al., 2024).

Conversely, areas with declining NPP are mainly in the northern and southern part of the island, as well as along the northeast coastal zone (Fig. 3). The decrease in NPP in the north and south is primarily associated with rapid socio-economic development and urban expansion. In the northeastern coastal region, the decline is mainly due to the degradation of coastal protection forests, driven by human activities such as agricultural reclamation, aquaculture, and infrastructure development.

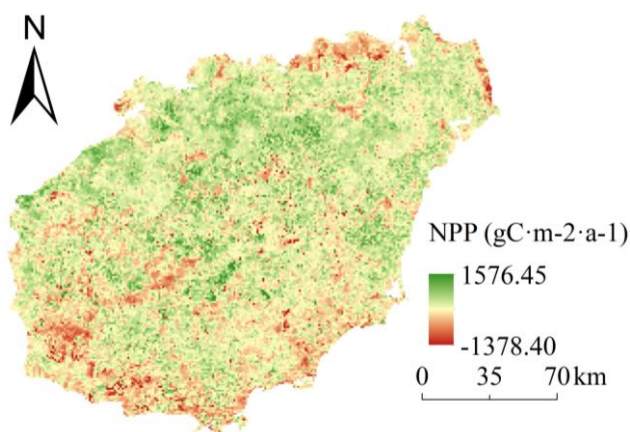


**Figure 3.** NPP variation distribution map of Hainan Island from 2000 to 2018

### ***Analysis of factors affecting NPP in Hainan Island***

#### ***Climate factors***

The climate data from 2000 to 2018 are summarized in *Table 2*. During the study period, the monthly average temperature in Hainan Island exhibited a pattern of initial increase followed by a slight decline. Meanwhile, the monthly total precipitation shown a steadily upward trend, while the monthly total solar radiation gradually decreased. Pearson correlation analysis indicates that the NPP of Hainan Island is significantly and positively correlated with monthly total precipitation, monthly average temperature, and monthly total solar radiation, with correlation coefficients of 0.871, 0.942, and 0.851, respectively. All correlations were statistically significant, suggesting that NPP in Hainan Island is jointly influenced by these three meteorological factors, with monthly average temperature exerting the strongest effect.

#### ***Land use change***

Between the period from 2000 to 2018 (*Table 4; Fig. 4*), the most significant expansion occurred in construction land, which increased by 532 km<sup>2</sup>. This expansion primarily came at the expense of cropland (49.31%), forestland (16.53%), and other

woodland (15.62%). Water bodies also experienced growth, largely due to conversion from cropland (29.5%) and grassland (14.75%). In contrast, cropland saw the largest reduction in area, decreasing by 354 km<sup>2</sup>, mainly being converted into construction land (41.92%) and other woodland (16.92%). Forestland also experienced substantial losses, primarily transitioning into other woodland (40.54%), cropland (20.61%), and construction land (18.24%).

The average NPP values for different land use types from 2000 to 2018, in descending order, are as follows: forestland (1863.40 gC m<sup>-2</sup> a<sup>-1</sup>), grassland (1100.56 gC m<sup>-2</sup> a<sup>-1</sup>), sparse woodland (1077.29 gC m<sup>-2</sup> a<sup>-1</sup>), cropland (1059.58 gC m<sup>-2</sup> a<sup>-1</sup>), other land (953.49 gC m<sup>-2</sup> a<sup>-1</sup>), water (933.95 gC m<sup>-2</sup> a<sup>-1</sup>), other woods (911.29 gC m<sup>-2</sup> a<sup>-1</sup>), tidal flat (904.95 gC m<sup>-2</sup> a<sup>-1</sup>), construction land (890.80 gC m<sup>-2</sup> a<sup>-1</sup>), and shrub (885.97 gC m<sup>-2</sup> a<sup>-1</sup>).

Given these NPP values, the observed land use changes generally resulted in a decline in ecosystem productivity. However, despite this, from a temporal perspective, the overall NPP of Hainan Island increased during the period, suggesting that the positive effect of climate change on NPP outweighed the negative impacts of land use change.

**Table 4.** Transfer matrix of LUCC in Hainan Island during 2000–2018 (unit: km<sup>2</sup>)

|      | Land-use types    | 2018     |             |       |                 |                |           |       |            |                   |            |
|------|-------------------|----------|-------------|-------|-----------------|----------------|-----------|-------|------------|-------------------|------------|
|      |                   | Cropland | Forest land | Shrub | Sparse woodland | Other woodland | Grassland | Water | Tidal flat | Construction land | Other land |
| 2000 | Cropland          | 8556     | 128         | 42    | 12              | 130            | 19        | 108   | 3          | 322               | 4          |
|      | Forest land       | 122      | 12786       | 16    | 15              | 240            | 44        | 45    | 0          | 108               | 2          |
|      | Shrub             | 53       | 21          | 2387  | 1               | 16             | 14        | 15    | 0          | 55                | 0          |
|      | Sparse woodland   | 21       | 16          | 6     | 874             | 27             | 3         | 10    | 0          | 21                | 0          |
|      | Other woodland    | 116      | 103         | 7     | 3               | 4681           | 4         | 33    | 1          | 102               | 0          |
|      | Grassland         | 15       | 54          | 10    | 3               | 19             | 1059      | 54    | 0          | 21                | 2          |
|      | Water             | 21       | 11          | 3     | 1               | 8              | 6         | 772   | 3          | 9                 | 0          |
|      | Tidal flat        | 6        | 0           | 0     | 0               | 0              | 1         | 45    | 62         | 4                 | 0          |
|      | Construction land | 39       | 15          | 3     | 4               | 11             | 0         | 49    | 0          | 656               | 0          |
|      | Other land        | 21       | 2           | 0     | 3               | 1              | 12        | 7     | 0          | 11                | 78         |

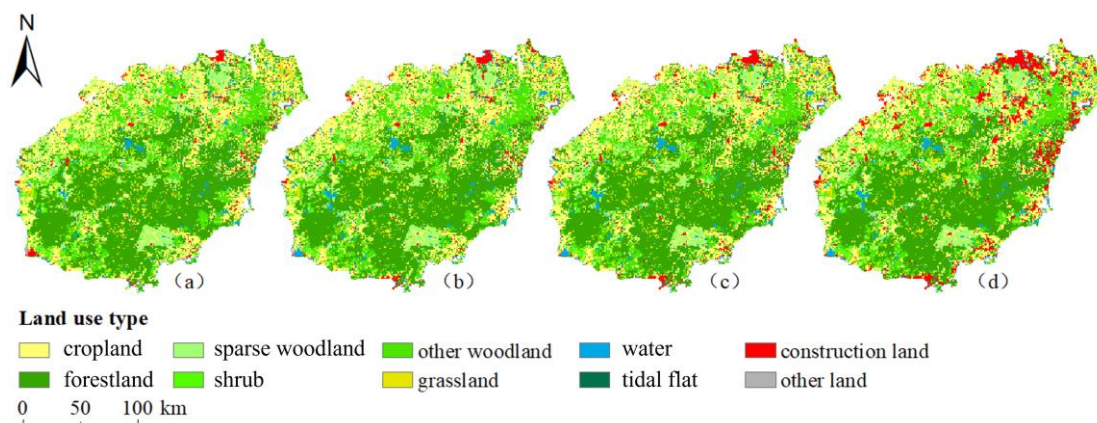


**Figure 4.** Land use of Hainan Island in 2000 (a), 2010 (b), 2018 (c), and 2050 (d)

### ***Future changes in land use and climate and their impact on NPP***

The main projected land use changes by 2050 are twofold: (1) forestland is increasingly being converted into construction land, cropland, and grassland. And (2) cropland is being largely replaced by construction land. Specifically, construction land is projected to increase by 1253 km<sup>2</sup>, and grassland by 120 km<sup>2</sup>. Conversely, cropland, forestland, and other forestlands are expected to decline by 706 km<sup>2</sup>, 360 km<sup>2</sup>, and 195 km<sup>2</sup>, respectively. When these shifts are analyzed in conjunction with the mean NPP values of the respective land categories, the simulation results indicate a decline in NPP due to future land use changes.

In terms of climate, compared to the baseline year of 2018, the projected changes in 2050 under the three climate scenarios SSP1-2.6, SSP2-4.5, and SSP5-8.5 are follows: the monthly average temperature increases by 1.23°C, 1.37°C and 1.65°C, respectively; monthly total precipitation is projected to change by +10.92%, +6.91% and +17.34%, and the monthly total solar radiation is anticipated to rise by 4.68%, 0.70% and 1.94%, respectively.

Under the combined influence of land use and climate change, the net primary productivity (NPP) of Hainan Island in 2050 is projected to decrease across all three scenarios, falling below the 2018 average of 1423.96 gC m<sup>-2</sup> a<sup>-1</sup>. The estimated NPP values for 2050 are 1346 gC m<sup>-2</sup> a<sup>-1</sup> under SSP1-2.6, 1315 gC m<sup>-2</sup> a<sup>-1</sup> under SSP2-4.5, and 1307 gC m<sup>-2</sup> a<sup>-1</sup> under SSP5-8.5 (*Fig. 5*).

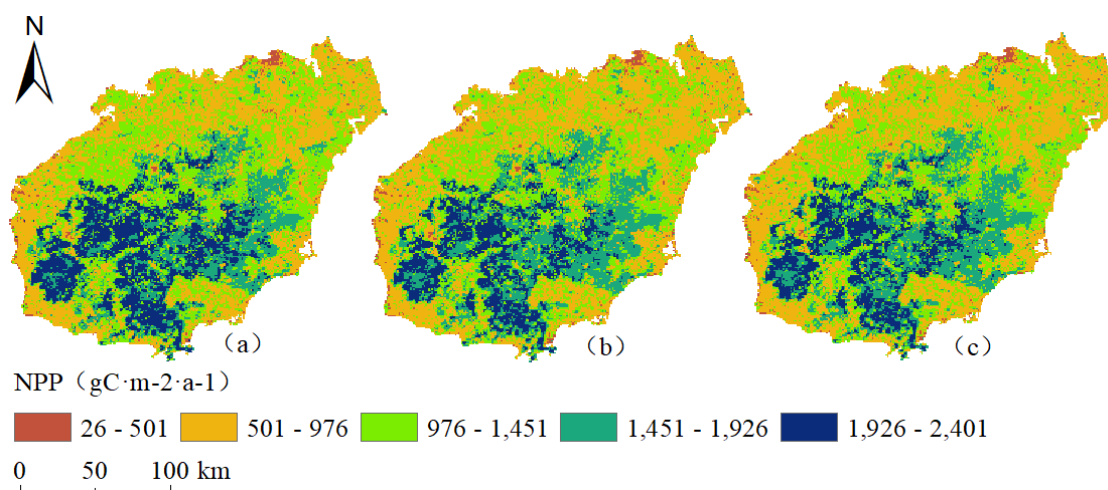


**Figure 5.** NPP in 2050 under three scenarios (a) SSP1-2.6, (b) SSP2-4.5 and (c) SSP5-8.5

As illustrated in *Figure 6*, the spatial distribution of NPP on Hainan Island from 2018 to 2050 indicates that areas experiencing a decrease in NPP under all three scenarios are predominantly concentrated in the central-eastern part of the island. In contrast, regions with increased NPP are mainly located along the southern and northern coastal areas. Among the three scenarios, the SSP1-2.6 scenario shows the greatest increase in NPP, while the SSP5-8.5 scenario leads to the most significant decrease in NPP.

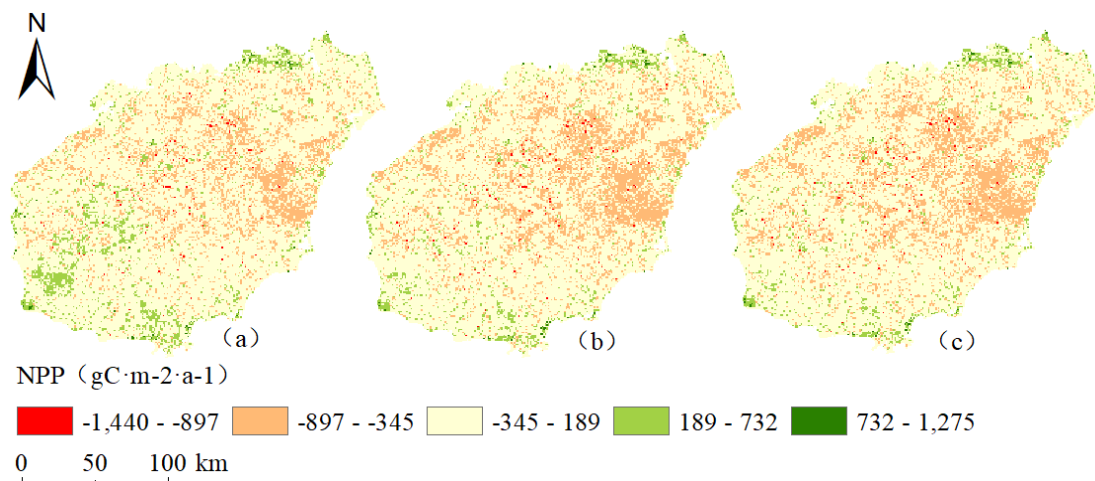


**Figure 6.** 2018-2050 NPP changes of three scenarios. (a) NPP change under SSP1-2.6 (b) NPP change under SSP2-4.5 (c) NPP change under SSP5-8.5

## Discussion

### *NPP responded to climate and land use change*

The mean NPP values for each land use type in this study are consistent with previous studies (Yang et al., 2021; Sun et al., 2022), confirming the reliability of the results. The analysis of NPP values indicates that various types of forest land and grassland play a crucial role in supporting the NPP function of Hainan Island. Among these, forestland has the highest average NPP value. Studies have shown that a decrease in forest NPP can significantly disrupt the carbon cycle (Corlett, 2016). Therefore, it is essential to strictly protect the forests of Hainan Island, particularly the forests in the central region, which serve as a critical ecological barrier for the island. Additionally, the potential for enhancing ecosystem services in urban construction areas should be explored, such as increasing the NPP on construction land by expanding urban green spaces. In conclusion, land use change is one of the primary factors influencing NPP variation on Hainan Island. However, the simulation of future land use changes in 2050 suggests that the increase in construction land and the decrease in forestland will remain the dominant trend, continuing to exert a negative impact on the island's NPP.

The NPP of Hainan Island in this study is positively correlated with the average temperature, precipitation and solar radiation, aligning with previous findings (Zhang et al., 2016; Xue et al., 2023; Ma et al., 2024). Across all three climate scenarios, temperature is projected to increase, while precipitation and solar radiation decrease, leading to a reduction in NPP. As NPP is sensitive to multiple factors, particularly temperature (Wang et al., 2024), it is crucial to emphasize the impact of temperature changes on NPP. This is especially important in tropical regions, where NPP is more significantly influenced by temperature fluctuations, drought, and precipitation variability (Luo et al., 2024).

Although land use changes on Hainan Island from 2000 to 2018 had a negative effect on NPP, overall NPP still increased under the influence of favorable climate conditions. However, under future scenarios, the east-central region of Hainan Island is projected to experience a notable decline in NPP, indicating heightened vulnerability. As such, targeted protection strategies are needed to preserve ecosystem productivity in this

region. Conversely, some areas particularly urban regions, are expected to see continued increases in NPP, suggesting a high degree of ecological resilience in Hainan's towns (Fig. 6).

### ***Sustainable development of social-ecological system***

Based on the SSP scenario simulations, future NPP changes on Hainan Island display significant variation across scenarios. The SSP1-2.6 scenario yields the highest average NPP value, reflecting a strong emphasis on environmental sustainability. However, it substantially compromises economic development goals, conflicting with the strategic objectives of constructing Hainan's Free Trade Port, thereby limiting its practical feasibility. In contrast, the SSP5-8.5 scenario presents the lowest average NPP value. Its development model, characterized by high resource consumption and excessive carbon emissions, poses serious threats to ecosystem functions and contradicts the ecological priorities outlined in the Ecological Civilization Pilot Zone strategy. The SSP2-4.5 scenario offers a balanced path, with a moderate average NPP value. It supports increased use of clean energy, reduced dependence on fossil fuels, and the integration of high-quality economic development with ecological conservation. This scenario not only helps maintain the stability of NPP functions but also aligns with Hainan's regional sustainable development objectives. Therefore, the SSP2-4.5 scenario provides a scientifically grounded framework for advancing the dual goals of Free Trade Port construction and the Ecological Civilization Pilot Zone strategy through the synergistic optimization of ecological and economic systems.

### ***Limitations***

There are inherent uncertainties in the quantitative assessment of NPP conducted in this study. First, the accuracy of meteorological data interpolation has been shown to significantly affect the reliability of NPP simulations (Shen et al., 2022). Second, extreme climatic events—such as droughts and heatwaves—introduce additional variability and elevate uncertainty in NPP estimates (Decuyper et al., 2020). Third, in tropical regions like Hainan Island, certain parameters are subject to further uncertainty due to persistent cloud cover and the “saturation” effect of vegetation indices, which limits their responsiveness to biomass variation (Piao et al., 2019). Despite these limitations, the methodology employed remains a viable approach for evaluating NPP dynamics under the influence of anthropogenic and climatic factors. It is evident that both human activities and climate change exert significant influence on NPP. However, given the complex interplay between these factors, future research should focus on improving methods to quantitatively distinguish their respective contributions to NPP variation.

### **Conclusion**

This study examines the spatial and temporal evolution of NPP on Hainan Island, analyzes its correlation with climate factors, simulates future NPP under different SSP-RCPs scenarios, and explores sustainable development pathways for tropical island social-ecological systems under climate change. The main conclusions are as follows:

(1) NPP on Hainan Island exhibits a spatial pattern characterized by “high in the center and low around the edges”. From 2000 to 2018, NPP showed a consistent upward

trend, with values increasing from 1199.90 gC m<sup>-2</sup> a<sup>-1</sup> in 2000 to 1250.86 gC m<sup>-2</sup> a<sup>-1</sup> in 2010 and 1447.83 gC m<sup>-2</sup> a<sup>-1</sup> in 2018.

(2) Among the different land use types, forestland had the highest average NPP, followed by grassland, open forestland, and cropland. NPP was significantly and positively correlated with total monthly precipitation, average monthly temperature, and total monthly solar radiation, with temperature exerting the strongest influence. Although land use changes from 2000 to 2018 led to a decline in NPP the compensatory effect of favorable climate conditions outweighed these negative impact, resulting in an overall increase in NPP.

(3) Under the combined effects of future climate and land use changes, NPP across all three SSP-RCP scenarios is projected to decline compared to 2018. However, the SSP2-4.5 scenario represents the most balanced development pathway, effectively integrating ecological protection with socio-economic development. This scenario provides a scientifically sound framework for supporting both the construction of Hainan's Free Trade Port and the advancement of the Pilot Ecological Civilization Zone strategy.

**Acknowledgments.** This research was financially supported by the National Science Found of China (No. 42371272), Hainan Provincial Natural Science Foundation of China (No.421RC1034), the Professor/Doctor Research Foundation of Huizhou University (No. 2022JB080), Guangdong Provincial Department of Education Characteristic Innovation Project (2024KTSCX092).

## REFERENCES

- [1] Arunrat, N., Sereenonchai, S., Chaowiwat, W., Wang, C. (2022): Climate change impact on major crop yield and water footprint under CMIP6 climate projections in repeated drought and flood areas in Thailand. – *Sci. Total Environ.* 807: 150741. <https://doi.org/10.1016/j.scitotenv.2021.150741>.
- [2] Camp, E. F., Schoepf, V., Suggett, D. J. (2018): How can “Super Corals” facilitate global coral reef survival under rapid environmental and climatic change? – *Glob. Chang. Biol.* 24: 2755-2757. <https://doi.org/10.1111/gcb.14153>.
- [3] Cao, D., Zhang, J. H., Xun, L., Yang, S. S., Wang, J. W., Yao, F. M. (2021): Spatiotemporal variations of global terrestrial vegetation climate potential productivity under climate change. – *Sci Total Environ.* 770. <https://doi.org/10.1016/j.scitotenv.2021.145320>.
- [4] Chen, L. Q., Wang, G. J., Miao, L. J., Gnyawali, K. R., Li, S. J., Amankwah, S. O. Y., Huang, J. L., Lu, J., Zhan, M. Y. (2021): Future drought in CMIP6 projections and the socioeconomic impacts in China. – *Int. J. Climatol.* 41: 4151-4170. <https://doi.org/10.1002/joc.7064>.
- [5] Chiaka, J. C., Yang, Q., Zhao, Y., Agostinho, F., Almeida, C. M. V. B., Giannetti, B. F., Li, H., Wu, M., Liu, G. (2024): Assessment of water-related ecosystem services and beneficiaries in the Hainan Tropical Rainforest National Park. – *Land (Basel)* 13: 1804. <https://doi.org/10.3390/land13111804>.
- [6] Corlett, R. T. (2016): The Impacts of Droughts in Tropical Forests. – *Trends Plant. Sci.* 21: 584-593. <https://doi.org/10.1016/j.tplants.2016.02.003>.
- [7] Decuyper, M., Chávez, R. O., Čufar, K., Estay, S. A., Clevers, J. G. P. W., Prislán, P., Gričar, J., Črepinšek, Z., Merela, M., de Luis, M., Notivoli, R. S., Del Castillo, E. M., Rozendaal, D. M. A., Bongers, F., Herold, M., Sass-Klaassen, U. (2020): Spatio-temporal assessment of beech growth in relation to climate extremes in Slovenia—an integrated

- approach using remote sensing and tree-ring data. – *Agric. For. Meteorol.* 287: 107925. <https://doi.org/10.1016/j.agrformet.2020.107925>.
- [8] Guo, L. H., Hao, C. Y., Wu, S. H., Gao, J. B., Zhao, D. S. (2016): Projected changes in vegetation net primary productivity of grassland in Inner Mongolia, China during 2011-2050. – *Chinese Journal of Applied Ecology* 27: 803-814.
- [9] Han, N. L., Zhang, Y. Q., Zhang, W. X. (2022): Simulation of temporal and spatial changes of land use and water yield in Hainan Island. – *Water Resources Protection* 38: 119-127.
- [10] Hernández-Delgado, E. A. (2015): The emerging threats of climate change on tropical coastal ecosystem services, public health, local economies and livelihood sustainability of small islands: cumulative impacts and synergies. – *Mar. Pollut. Bull.* 101: 5-28. <https://doi.org/10.1016/j.marpolbul.2015.09.018>.
- [11] Jiang, T., Wang, A. J., Su, B. D., Zhai, J. Q., Tao, H., Jing, C., Huang, J. L., Wen, S. S., Pan, J. Y. (2020): Perspectives of human activities in global climate change: evolution of socio-economic scenarios. – *Journal of Nanjing University of Information Science and Technology (Natural Science Edition)* 12: 68-80.
- [12] Khelifa, R., Mahdjoub, H., Samways, M. J. (2022): Combined climatic and anthropogenic stress threaten resilience of important wetland sites in an arid region. – *Sci. Total Environ.* 806: 150806. <https://doi.org/10.1016/j.scitotenv.2021.150806>.
- [13] Kumar, M., Savita, Singh, H., Pandey, R., Singh, M. P., Ravindranath, N. H., Kalra, N. (2019): Assessing vulnerability of forest ecosystem in the Indian Western Himalayan region using trends of net primary productivity. – *Biodivers. Conserv.* 28: 2163-2182. <https://doi.org/10.1007/s10531-018-1663-2>.
- [14] Li, C. H., Wang, Y. T., Wu, X. D., Cao, H. J., Li, W. P., Wu, T. H. (2021a): Reducing human activity promotes environmental restoration in arid and semi-arid regions: a case study in Northwest China. – *Sci. Total Environ.* 768: 144525. <https://doi.org/10.1016/j.scitotenv.2020.144525>.
- [15] Li, X. C., Luo, Y. H., Wu, J. S. (2022): Decoupling relationship between urbanization and carbon sequestration in the Pearl River Delta from 2000 to 2020. – *Remote Sens. (Basel)* 14: 526. <https://doi.org/10.3390/rs14030526>.
- [16] Li, X. Y., Guo, J. M., Qi, S. Z. (2021b): Forestland landscape change induced spatiotemporal dynamics of subtropical urban forest ecosystem services value in forested region of China: a case of Hangzhou City. – *Environ. Res.* 193: 110618. <https://doi.org/10.1016/j.envres.2020.110618>.
- [17] Linger, E., Hogan, J. A., Cao, M., Zhang, W. F., Yang, X. F., Hu, Y. H. (2020): Precipitation influences on the net primary productivity of a tropical seasonal rainforest in Southwest China: a 9-year case study. – *For. Ecol. Manage.* 467: 118153. <https://doi.org/10.1016/j.foreco.2020.118153>.
- [18] Liu, G. B., Shao, Q. Q., Fan, J. W., Ning, J., Rong, K., Huang, H. B., Liu, S. C., Zhang, X. Y., Niu, L. N., Liu, J. Y. (2022): Change trend and restoration potential of vegetation net primary productivity in China over the past 20 years. – *Remote Sens. (Basel)* 14: 1634. <https://doi.org/10.3390/rs14071634>.
- [19] Liu, X. P., Liang, X., Li, X., Xu, X. C., Ou, J. P., Chen, Y. M., Li, S. Y., Wang, S. J., Pei, F. S. (2017): A future land use simulation model (FLUS) for simulating multiple land use scenarios by coupling human and natural effects. – *Landsc. Urban Plan.* 168: 94-116. <https://doi.org/10.1016/j.landurbplan.2017.09.019>.
- [20] Luo, M., Meng, F., Sa, C., Bao, Y., Liu, T., De Maeyer, P. (2024): Detecting drought-related temporal effects on global net primary productivity. – *Remote Sens.* 16: 3787. <https://doi.org/10.3390/rs16203787>.
- [21] Piao, S. L., Zhang, X. P., Chen, A. P., Liu, Q., Lian, X., Wang, X. H., Peng, S. S., Wu, X. C. (2019): The impacts of climate extremes on the terrestrial carbon cycle: a review. – *Science China Earth Sciences* 62: 1551-1563. <https://doi.org/10.1007/s11430-018-9363-5>.

- [22] Raty, O., Raisanen, J., Ylhaisi, J. S. (2014): Evaluation of delta change and bias correction methods for future daily precipitation: intermodel cross-validation using ENSEMBLES simulations. – *Clim. Dyn.* 42: 2287-2303. <https://doi.org/10.1007/s00382-014-2130-8>.
- [23] Rawat, M., Singh, R., Sharma, J., Saklani, H., Chand, T., Bhatt, I. D., Pandey, R. (2022): An overview of the functioning of temperate forest ecosystems with particular reference to Himalayan temperate forest. – *Trees, Forests and People* 8: 100230. <https://doi.org/10.1016/j.tfp.2022.100230>.
- [24] Reichstein, M., Bahn, M., Ciais, P., Frank, D., Mahecha, M. D., Seneviratne, S. I., Zscheischler, J., Beer, C., Buchmann, N., Frank, D. C., Papale, D., Rammig, A., Smith, P., Thonicke, K., van der Velde, M., Vicca, S., Walz, A., Wattenbach, M. (2013): Climate extremes and the carbon cycle. – *Nature* 500: 287-295. <https://doi.org/10.1038/nature12350>.
- [25] Shen, X., Liu, Y., Zhang, J., Wang, Y., Ma, R., Liu, B., Lu, X., Jiang, M. (2022): Asymmetric impacts of diurnal warming on vegetation carbon sequestration of marshes in the Qinghai Tibet Plateau. – *Global Biogeochem. Cycles* <https://doi.org/10.1029/2022GB007396>.
- [26] Sun, C. J., Qiao, P., Jiarui, W., Wang, H. Y., Sun, J. L. (2022): Spatio-temporal variation characteristics of net primary productivity in Lvliang contiguous poverty areas since 2000. – *Acta Ecologica Sinica* 1-10.
- [27] Tian, X. N., Chen, Y., Chen, X. W., Gao, L. (2022): Estimation of the future runoff in the Jinjiang watershed based on FLUS and SSPs scenarios. – *Journal of Chian Hydrology* 1-12.
- [28] Wang, M., Sun, K., Jia, J. J., Wu, F., Gao, Y. (2024): Climate change drove the decline in yangtze estuary net primary production over the past two decades. – *Environmental Science & Technology* 58(43): 19305-19314.
- [29] Wang, Y. S., Gu, J. D. (2021): Ecological responses, adaptation and mechanisms of mangrove wetland ecosystem to global climate change and anthropogenic activities. – *Int. Biodeterior. Biodegradation* 162: 105248. <https://doi.org/10.1016/j.ibiod.2021.105248>.
- [30] Wang, Z., Li, X., Mao, Y., Li, L., Wang, X., Lin, Q. (2022): Dynamic simulation of land use change and assessment of carbon storage based on climate change scenarios at the city level: a case study of Bortala, China. – *Ecol. Indic.* 134: 108499. <https://doi.org/10.1016/j.ecolind.2021.108499>.
- [31] Xu, C. G., McDowell, N. G., Fisher, R. A., Wei, L., Sevanto, S. N., Christoffersen, B. O., Weng, E. S., Middleton, R. S. (2019): Increasing impacts of extreme droughts on vegetation productivity under climate change. – *Nat. Clim. Chang.* 9: 948-953. <https://doi.org/10.1038/s41558-019-0630-6>.
- [32] Xue, P., Liu, H. Y., Zhang, M. Y., Gong, H. B., Cao, L. (2022): Nonlinear characteristics of NPP based on ensemble empirical mode decomposition from 1982 to 2015—a case study of six coastal provinces in Southeast China. – *Remote Sens. (Basel)* 14: 15. <https://doi.org/10.3390/rs14010015>.
- [33] Xue, S., Guo, X., He, Y., Cai, H., Li, J., Zhu, L., Ye, C. (2024): Effects of future climate and land use changes on runoff in tropical regions of China. – *Sci. Rep.* 14. <https://doi.org/10.1038/s41598-024-81754-8>.
- [34] Yang, H., Huang, J. L., Liu, D. F. (2020): Linking climate change and socioeconomic development to urban land use simulation: analysis of their concurrent effects on carbon storage. – *Appl. Geogr.* 115: 102135. <https://doi.org/10.1016/j.apgeog.2019.102135>.
- [35] Yang, H. F., Zhong, X. N., Deng, S. Q., Xu, H. (2021): Assessment of the impact of LUCC on NPP and its influencing factors in the Yangtze River basin, China. – *Catena (Amst)* 206: 105542. <https://doi.org/10.1016/j.catena.2021.105542>.
- [36] Yuan, Q. Z., Wu, S. H., Dai, E. F., Zhao, D. S., Ren, P., Zhang, X. R. (2016): NPP vulnerability of China's potential vegetation to climate change in the past 50 years. – *Acta Geographica Sinica* 71: 797-806.

- [37] Zhang, H. Y., Hobbie, E. A., Feng, P. Y., Niu, L. A., Hu, K. L. (2022b): Can conservation agriculture mitigate climate change and reduce environmental impacts for intensive cropping systems in North China Plain? – *Sci. Total Environ.* 806: 151194. <https://doi.org/10.1016/j.scitotenv.2021.151194>.
- [38] Zhang, L. X., Chen, X. L., Xin, X. G. (2019): Short commentary on CMIP6 scenario model intercomparison project (ScenarioMIP). – *Climate Change Research* 15(5): 519-525.
- [39] Zhang, M., Yuan, N. Q., Lin, H., Liu, Y., Zhang, H. Q. (2022a): Quantitative estimation of the factors impacting spatiotemporal variation in NPP in the Dongting Lake wetlands using Landsat time series data for the last two decades. – *Ecol. Indic.* 135: 108544. <https://doi.org/10.1016/j.ecolind.2022.108544>.
- [40] Zhang, Y., Zhang, C. B., Wang, Z. Q., Chen, Y. Z., Gang, C. C., An, R., Li, J. L. (2016): Vegetation dynamics and its driving forces from climate change and human activities in the Three-River Source Region, China from 1982 to 2012. – *Sci. Total Environ.* 563-564: 210-220. <https://doi.org/10.1016/j.scitotenv.2016.03.223>.
- [41] Zhu, W. Q., Pan, Y. Z., He, H., Yu, D. Y., Hu, H. B. (2006): Simulation of maximum light utilization rate of typical vegetation in China. – *Chinese Science Bulletin* 700-706.
- [42] Zhu, W. Q., Pan, Y. Z., Zhang, J. S. (2007): Estimation of net primary productivity of Chinese terrestrial vegetation based on remote sensing. – *Journal of Plant Ecology* 31(3): 413-424.